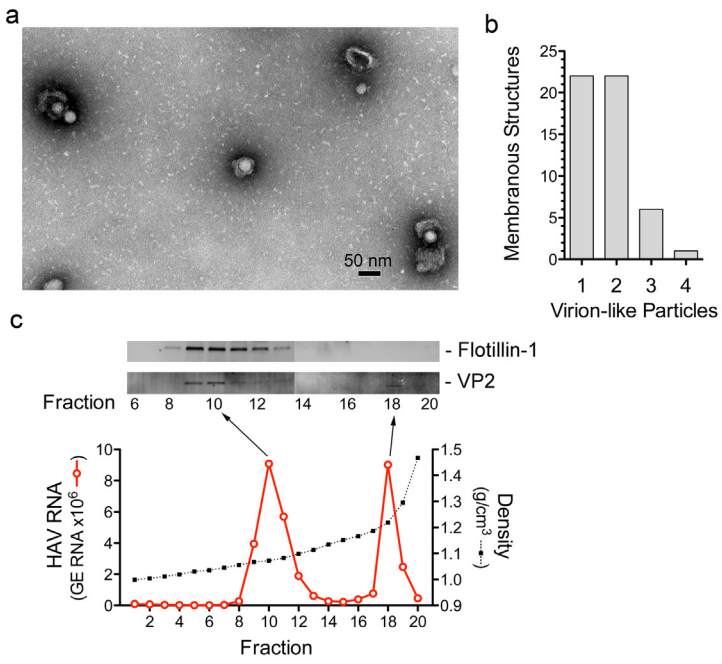

Supplementary Figure 1 | a, Transmission electron microscopic image of negatively-stained eHAV particles in a fraction from an isopycnic iodixanol gradient with a density of 1.080 g/cm^3. Magnification = x100,000. **b,** Distribution of the number of virion-like particles contained within individual membranous structures. **c,** Distribution of flotillin-1 and the HAV capsid protein VP2 in fractions of an iodixanol gradient, as determined by immunoblotting. Shown for comparison is the HAV RNA in fractions, determined as in Fig. 1b in the main manuscript.

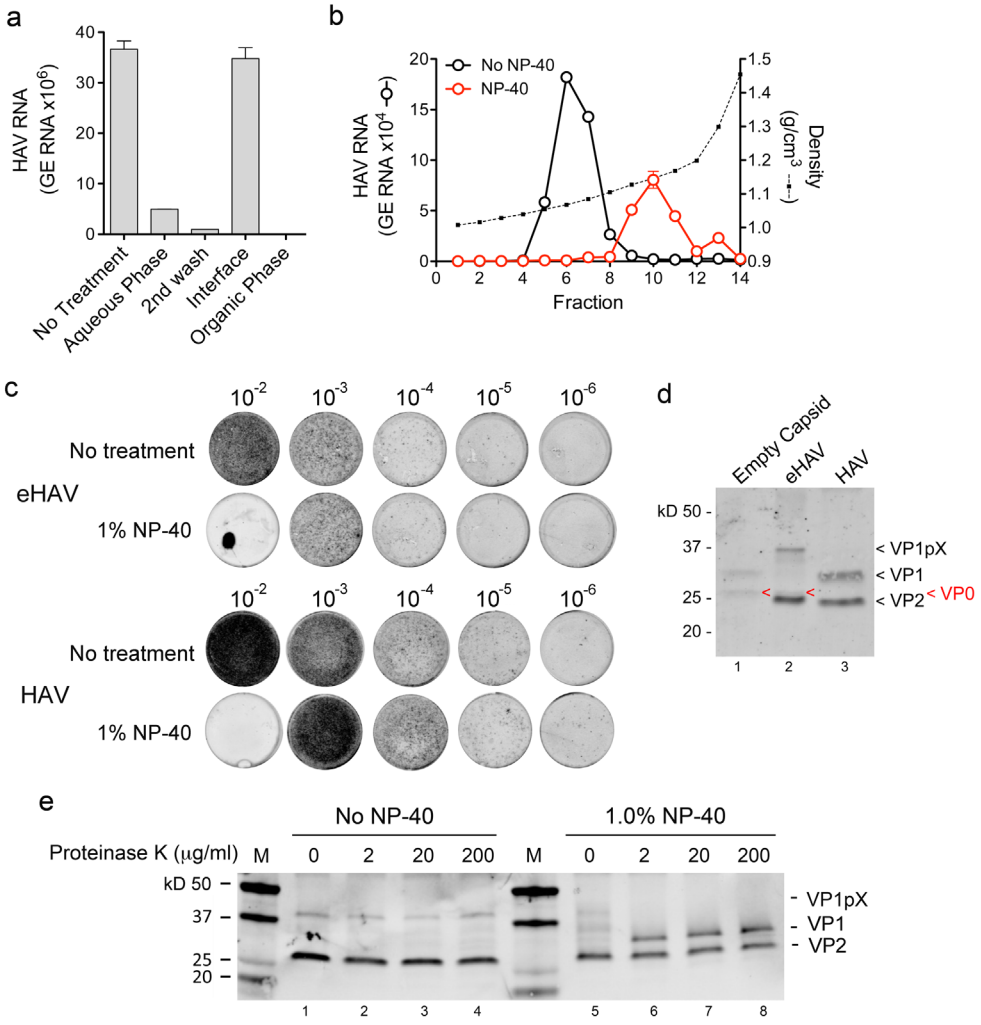

Supplementary Figure 2 | a, Gradient-purified eHAV was extracted with an equal volume of chloroform, and the interface plus lower organic phase subsequently back-extracted twice with water. RNA was extracted from the initial aqueous phase, the second wash, the final interface and organic phase and subjected to qRT-PCR analysis. **b,** Gradient purified eHAV was treated or not treated with 1% NP-40 prior to being subjected to isopycnic ultracentrifugation in iodixanol gradients. HAV RNA in gradient fractions was measured by qRT-PCR. **c,** eHAV remains infectious following treatment with 1% NP-40. Iodixanol gradient fractions containing eHAV (top) or non-enveloped HAV particles (bottom) were treated with 1% NP-40 as in panel b, diluted in medium as indicated, and inoculated onto cells for titration of infectivity by IR-FIFA. Note that NP-40 remained toxic to cells at the 10^{-2} dilution. **d,** Immunoblot of empty capsids (which are present in low abundance in infected cells and were recovered from a rate-zonal sucrose gradient), eHAV, and nonenveloped HAV (from an iodixanol gradient) with anti-VP1 and anti-VP2 peptide antibodies. Proteins were separated by SDS-PAGE on a 12% gel. Note the presence of unprocessed VP0 (predicted mass 27.0-27.3 kD) in empty capsids (red marker), while most VP0 has been processed to VP2 (24.9 kD) in eHAV. **e,** NP-40 treatment renders pX present in eHAV susceptible to proteinase K digestion. Iodixanol gradient-purified eHAV was treated with 1% NP-40 for 15 min, then placed in increasing concentrations of proteinase K with 2 mM $CaCl_2$ at 37° C for 30 min. Reactions were stopped by the addition of 10 mM phenylmethylsulfonyl fluoride and samples separated on 4-20% SDS-PAGE followed by immunoblotting with anti-VP1 and anti-VP2.

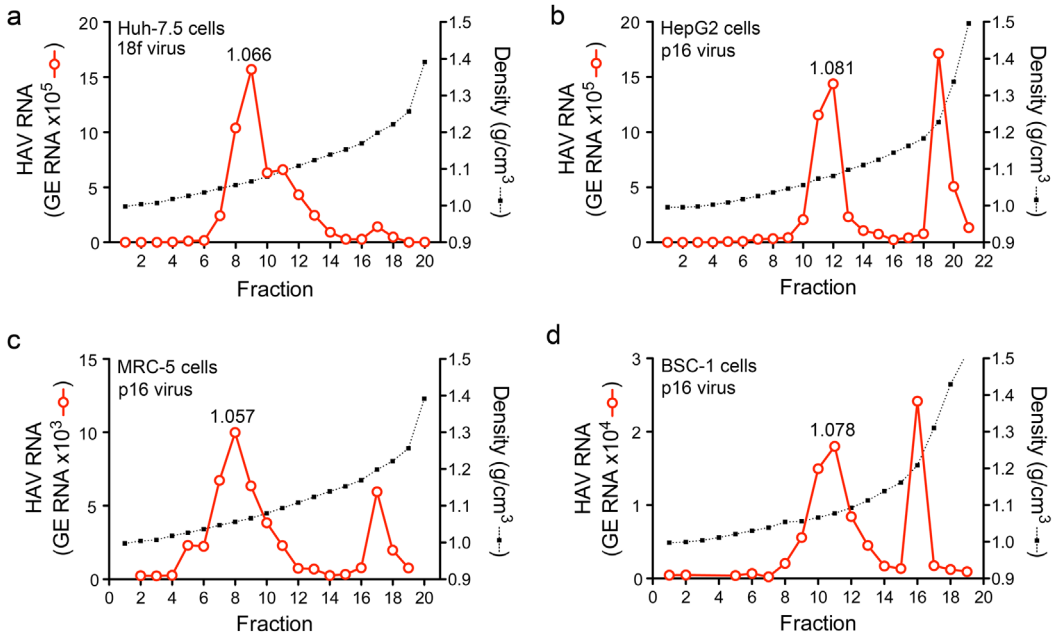

Supplementary Figure 3. | Buoyant densities of (**a**) cytopathic HM175/18f virus and (**b-d**) low-passage, non-cytopathic HM175/p16 virus released into supernatant fluids of infected **a**, Huh-7.5, **b**, HepG2, **c**, MRC-5, and **d**, BSC-1 cells. Virus in supernatant culture fluids was centrifuged to equilibrium on iodixanol gradients, and HAV RNA detected in fractions by RT-PCR, as in Fig. 1b. eHAV banding at a density of 1.057-1.081 gm/cm^3 was detected in gradient fractions from each cell type at varying proportions of the total virus yield.

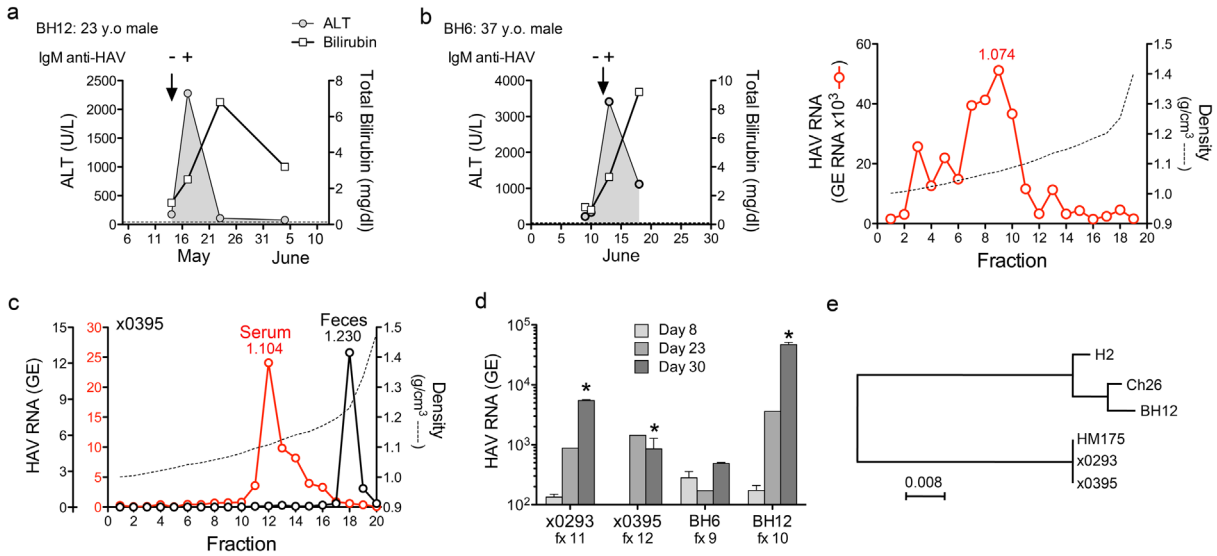

Supplementary Figure 4. | **a,** Clinical course of patient BH12, from whom serum was collected (arrow) prior to IgM anti-HAV seroconversion. ALT = serum alanine aminotransferase. Bilirubin = total serum bilirubin. Density gradient centrifugation of virus present in the initial serum specimen is shown in Fig. 2a. **b,** (left) Similar clinical profile of patient BH6. (right) Buoyant density of HAV particles in serum from patient BH6, collected on the date indicated by the arrow in the left-hand panel. **c,** Buoyant density of HAV particles in serum and feces of a chimpanzee infected with wild-type HM175 virus, x0395[5]. HAV RNA in gradient fractions was quantified by qRT-PCR. Fecal HAV RNA is $x10^5$, while plasma RNA is $x10^2$. **d,** Isolation of wild-type HAV from peak fractions (fx) of gradients containing eHAV from chimpanzee (x0293, Fig. 2b, and x0395, panel c) and human (BH6, panel b, right, and BH12, Fig. 2a) sources. Aliquots of fractions from gradients loaded with serum or plasma samples were inoculated onto Huh-7.5 cells, and supernatant fluids collected 8, 23, and 30 days after inoculation were assayed for HAV RNA by qRT-PCR. "*" indicates samples from which viral RNA in 30 day supernatant fluids was amplified by RT-PCR and sequenced. **e,** Neighbor-joining tree showing nucleotide sequence relatedness of eHAV isolates in the VP1-2B region (nts 2902-3272) relative to reference strains. BH12 virus (GenBank KC245088) is a genotype 1a isolate closely related to Ch-26 (AB643802.1) and H2 (EF406357.1) viruses identified in Japan. Virus isolated from the chimpanzee samples was identical in sequence to HM175 virus (M14707.1, genotype 1b), the inoculum used to infect these animals[5].

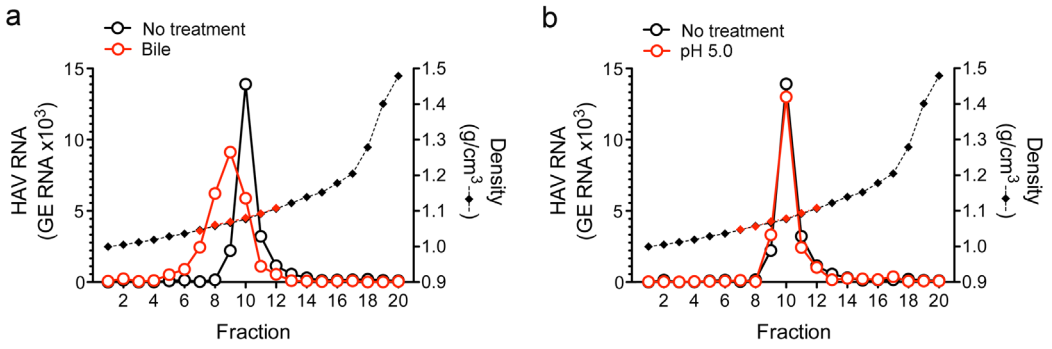

Supplementary Figure 5. | Physical stability of eHAV. **a,** Buoyant density of gradient-purified eHAV particles in an iodixanol density gradient following suspension in 90% porcine bile for 2 hrs at 37° C. Viral RNA was detected within gradient fractions by RT-PCR, and the results plotted superimposed on a companion gradient loaded with untreated eHAV. In replicate independent experiments, suspending eHAV in up to 98% porcine bile did not result in conversion to nonenveloped virions. **b,** Buoyant density of eHAV particles incubated in media for 15 min at a pH of 5.0. Experimental details were otherwise as described for panel a. Exposure to pH 5.0 resulted in no change in the buoyant density of eHAV.

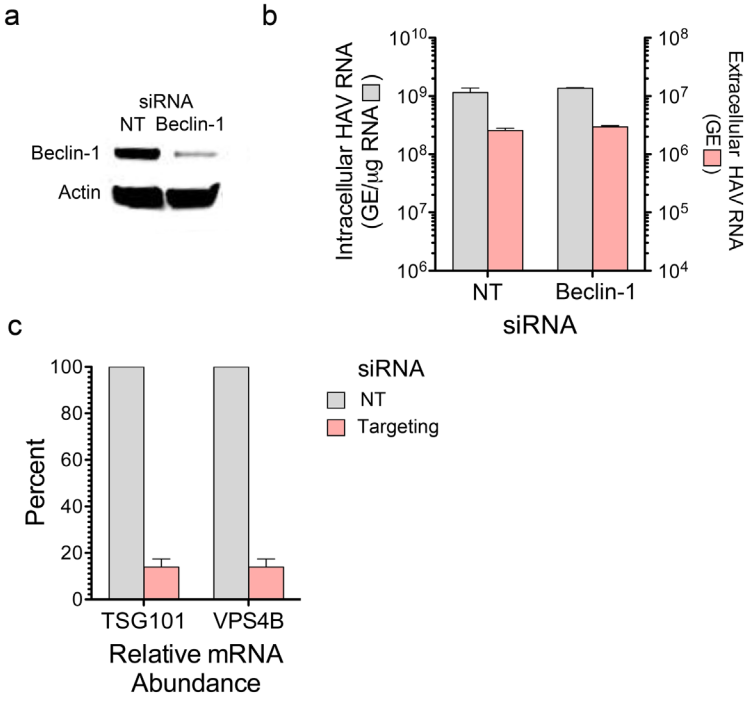

Supplementary Figure 6. | **a,** Immunoblot showing efficiency of beclin-1 knockdown 72 hrs after transfection of HM175/p16-infected Huh-7.5 cells with beclin-1-specific and non-targeting (NT) siRNAs. Actin was included as a loading control. **b,** Intracellular and extracellular HAV RNA as determined by qRT-PCR 72 hrs after transfection of the indicated siRNAs. **c,** qRT-PCR analysis of the knockdown efficiency of TSG101 and VPS4B siRNAs.

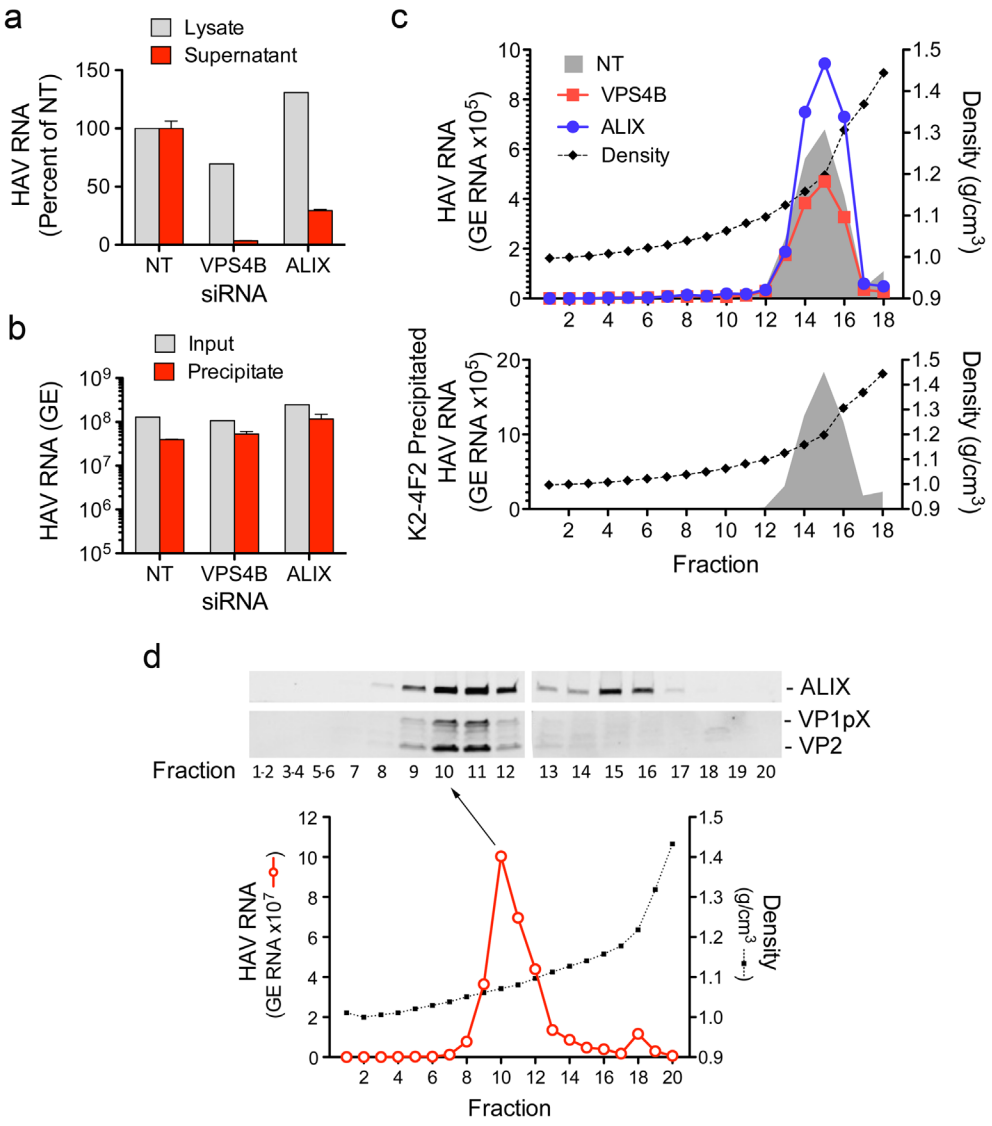

Supplementary Figure 7. | HAV capsid formation in VPS4B- and ALIX-depleted cells. **a,** HAV RNA content of cell lysates and supernatant fluids 3 days after infection of VPS4B- and ALIX-depleted cells (m.o.i. =10). Cells were transfected with NT, VPS4B- and ALIX-specific siRNAs 2 days prior to infection, and lysed at harvest in the presence of detergent. Results are shown as percent RNA measured by qRT-PCR in lysates (normalized to total protein) or supernatant fluids relative to NT siRNA-transfected cells. **b,** HAV RNA precipitated from 200 µl of cell lysates in panel a with the capsid-specific mAb, K24F2. Abundant HAV RNA precipitated from lysates of VPS4B and ALIX-depleted cells indicates continued capsid assembly. **c**, (top) Iodixanol density gradient centrifugation of lysates from panel a. (bottom) K24F2-precipitation of HAV RNA in fractions from the iodixanol gradient loaded with the control NT lysate confirms that the intracellular RNA banding within fractions 14-16 is packaged within HAV capsids. **d,** Immunoblots showing that ALIX co-distributes with VP1pX and VP2 in fractions of an iodixanol gradient loaded with supernatant fluid from p16 virus-infected cells. HAV RNA distribution is shown below.

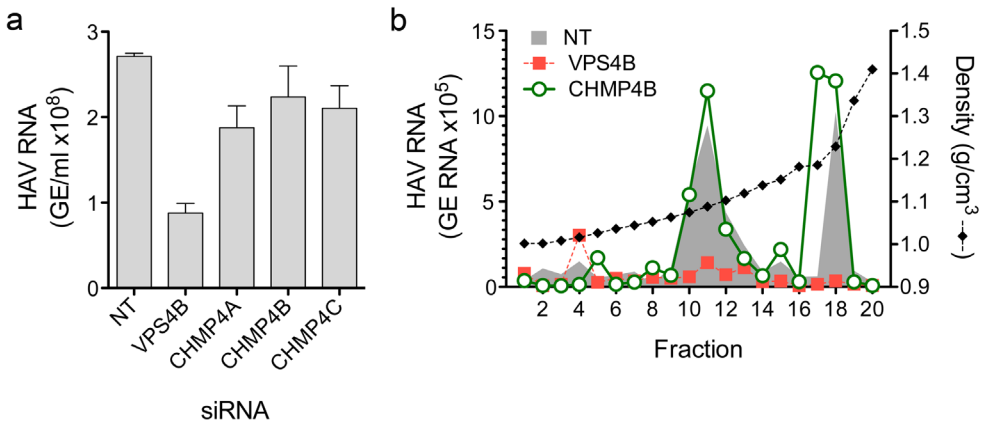

Supplementary Figure 8. | eHAV release following siRNA-mediated depletion of CHMP4 proteins. **a.** Total HAV RNA released into supernatant fluids hrs by p16 virus-infected cells 37-72 hrs after transfection of the indicated gene-specific or non-targeting (NT) siRNA. Results shown represent mean ± s.e.m. HAV RNA copies/ml released into media from replicate cell cultures. Knockdown efficiency was assessed by comparison of mRNA copy numbers in lysates of cells transfected with gene-specific vs. NT siRNAs and ranged from 81-84% for the 3 CHMP4 genes at 72 hrs. **b.** To confirm that CHMP4B depletion does not impair eHAV release, supernatant culture fluids collected from siRNA-transfected cells in an independent experiment were layered onto pre-formed iodixanol gradients and spun to equilibrium as in Fig. 1b of the main manuscript. HAV RNA was assayed in aliquots of individual gradient fractions by RT-PCR.

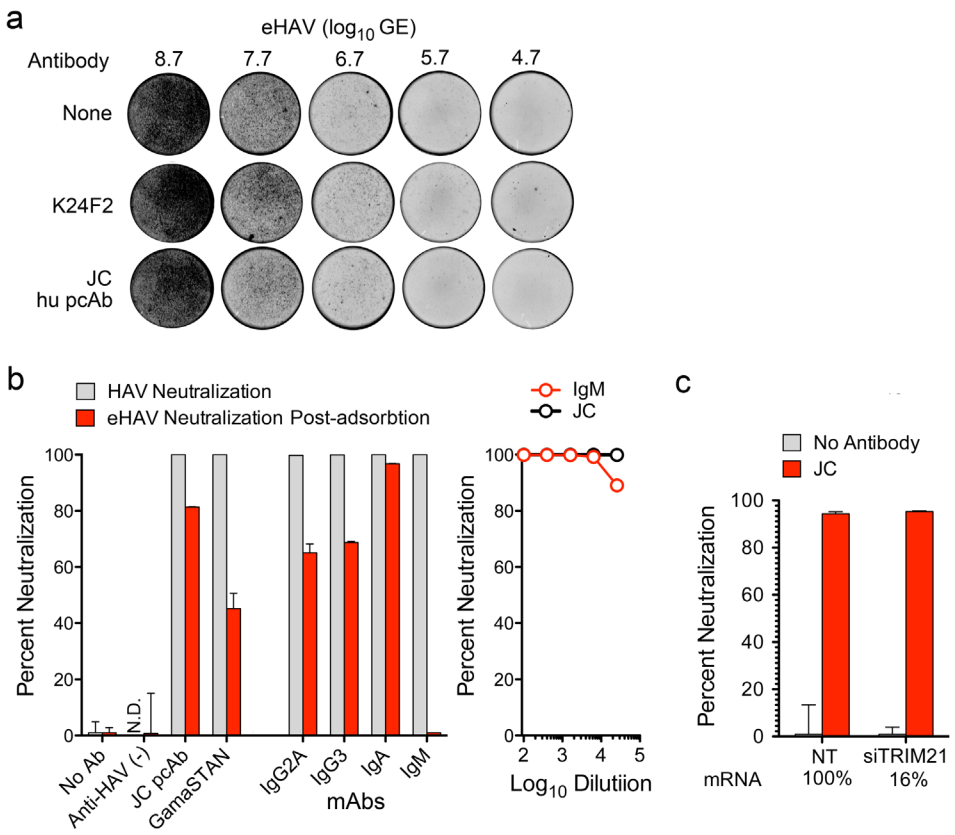

Supplementary Figure 9. | Antibody-mediated neutralization of eHAV. **a,** IR-FIFA showing a lack of neutralization of successive 10-fold dilutions of gradient-purified eHAV with the mAb K24F2 or JC, a human convalescent plasma sample with potent polyclonal HAV neutralizing activity. Neutralization was carried out as in Fig. 1g. **b,** (left) Relative efficiency of antibody-mediated neutralization of non-enveloped HAV in a standard neutralization assay (mixing of antibody with virus prior to inoculating cells) vs. neutralization of eHAV when antibody was added to medium 4 hrs after removal of the inoculum and washing of the cell sheet. Similar results were obtained when antibody was added immediately after inoculum removal. In both assays, cells were harvested 72 hrs after inoculum removal and intracellular HAV RNA abundance was determined by qRT-PCR. Results are shown as percent reduction in HAV RNA, ± s.e.m. in replicate assays. "Anti-HAV (-)" represents summary results from 5 human sera that were negative for anti-HAV by ELISA. "GamaSTAN" (GamaSTAN S/D, Talecris Biotherapeutics) is a commercially available 15-18% protein solution of pooled human immunoglobulin, solubilized Cohn fraction II, that is approved for use in humans for post-exposure prophylaxis against hepatitis A. Murine monoclonal antibodies (mAbs) were used at a 1:100 dilution: K32F2 (IgG2A), H10 (IgG3), 1.193 (IgA), and H14C42 (IgM), each of which recognizes an HAV capsid epitope[24]. (right) Nonenveloped HAV neutralization by serial dilutions of the polyclonal antibody, JC, and H14C42 (IgM). **c,** siRNA knockdown of TRIM21 does not impair neutralization of eHAV by JC human antibody added to medium following virus adsorption, as in panel b. Shown below each column is the percent TRIM21 mRNA determined by qRT-PCR compared to nontargeting (NT) siRNA transfected cells at the time of cell harvest.

Supplementary Table 1. Sequences of gene-targeting siRNA pools.

Gene	On-TARGETplus SMARTpool siRNA
TSG101	5′-CCGUUUAGAUCAAGAAGUA-3′
	5′-CUCCAUACCCAUCCGGAUA-3′
	5′-CCACAACAAGUUCUCAGUA-3′
	5′-CCAAAUACUUCCUACAUGC-3′
HRS	5′-GAGGUAAACGUCCGUAACA-3′
	5′-GCACGUCUUUCCAGAAUUC-3′
	5′-AAAGAACUGUGGCCAGACA-3′
	5′-GAACCCACACGUCGCCUUG-3′
VPS4B	5′-UCAAGGUGCCAUUGUUAUA-3′
	5′-CUACUUAGCCAAAGCUGUA-3′
	5′-CGAUAGAUCUGGCUAGCAA-3′
	5′-GGGCAAAGUGUACAGAAUA-3′
ALIX	5′-CAGAUCUGCUUGACAUUUA-3′
	5′-UCGAGACGCUCCUGAGAUA-3′
	5′-GCGUAUGGCCAGUAUAAUA-3′
	5′-GUACCUCAGUCUAUAUUGA-3′
TRIM21	5′-GCAGCACGCUUGACAAUGA-3′
	5′-AAUAUUGGAUCACAAGGAU-3′
	5′-UCUCAGAGCUAGAUCGAAG-3′
	5′-GAAUGUGCCUUUACAGGAC-3′
Beclin-1	5′-GAUACCGACUUGUUCCUUA-3′
	5′-GGAACUCACAGCUCCAUUA-3′
	5′-CUAAGGAGCUGCCGUUAUA-3′
	5′-GAGAGGAGCCAUUUAUUGA-3′
CHMP4A	5′-CCCUGGAGUUUCAGCGUGA-3′
	5′-GGAAGAAAAGAUUCGAACA-3′
	5′-UGUUAAAUGUGGGCGACAA-3′
	5′-GGCACAAACUGACGGGACA-3′
CHMP4B	5′-CCAUCGAGUUCCAGCGGGA-3′
	5′-AGAAGAGUUUGACGAGGAU-3′
	5′-CGGAAGAGAUGUUAAGCAA-3′
	5′-UGGAAAGGGUCGACUGGUU-3′